Carrier Phase Estimation Methods in Coherent Transmission Systems Influenced by Equalization Enhanced Phase Noise

Tianhua Xu[a,b,c*], Gunnar Jacobsen[b], Sergei Popov[a], Jie Li[b], Ari T. Friberg[a], Yimo Zhang[c]

[a]Royal Institute of Technology, Stockholm, SE-16440, Sweden

[b]Acreo AB, Electrum 236, SE-16440, Kista, Sweden

[c]Tianjin University, Tianjin, 300072, P.R. China

Email: tianhua@kth.se

Telephone number: +46-762178043

Fax: +46-87896672

Mail address: Optics Group, KTH-Electrum 229, Kista, Stockholm, SE-16440, Sweden

[*] Corresponding author: E-mail address: tianhua@kth.se; telephone number: +46-762178043; fax: +46-87896672

ABSTRACT

We present a comparative study on three carrier phase estimation algorithms, including a one-tap normalized least mean square (NLMS) method, a block-average method, and a Viterbi-Viterbi method in the *n*-level phase shift keying coherent transmission systems considering the equalization enhanced phase noise (EEPN). In these carrier phase estimation methods, the theoretical bit-error-rate floors based on traditional leading-order Taylor expansion are compared to the practical simulation results, and the tolerable total effective linewidths (involving the transmitter, the local oscillator lasers and the EEPN) for a fixed bit-error-rate floor are evaluated with different block size, when the fiber nonlinearities are neglected. The complexity of the three carrier phase estimation methods is also discussed. We find that the carrier phase estimation methods in practical systems should be analyzed based on the simulation results rather than the traditional theoretical predictions, when large EEPN is involved. The one-tap NLMS method can always show an acceptable behavior, while the step size is complicated to optimize. The block-average method is efficient to implement, but it behaves unsatisfactorily when using a large block size. The Viterbi-Viterbi method can show a small improvement compared to the block-average method, while it requires more computational complexity.

Key Words: Coherent optical transmission system, carrier phase estimation, equalization enhanced phase noise, phase shift keying

PACS: 42.25.Kb, 42.79.Sz

1. INTRODUCTION

Optical impairments such as chromatic dispersion (CD), polarization mode dispersion (PMD), phase noise (PN) and nonlinear effects degrade the performance of high speed optical fiber transmission systems severely [1-4]. Coherent optical receivers allow the significant equalization of transmission system impairments in the electrical domain, where the fiber dispersion and carrier phase noise can be well compensated by the efficient digital signal processing (DSP) [5-8]. Several feed-forward and feed-back carrier phase estimation (CPE) algorithms have been validated as the effective methods for mitigating the phase fluctuation from the laser sources [9-13]. However, in these algorithms, the analysis of the phase noise in the transmitter (TX) and the local oscillator (LO) lasers is often lumped together, and the interaction between the large chromatic dispersion and the laser phase noise is neglected.

The complicated interplay between the electronic CD equalization and the laser phase noise has been investigated in recent work, and this leads to an effect of equalization enhanced phase noise (EEPN) [14-24]. W. Shieh, K. P. Ho and A. P. T. Lau et al. have provided the theoretical evaluation for the EEPN based on the enhancement of the LO phase noise due to the dispersion equalization, and they also analyzed the EEPN induced time jitter in coherent systems [14-17]. C. Xie has investigated the influence of large CD on the LO phase noise to amplitude noise conversion, and the impact of large CD on the fiber nonlinear effects [18,19]. I. Fatadin and S. J. Savory have studied the impacts of the EEPN in quadrature phase shift keying (QPSK), 16-level quadrature amplitude modulation (16-QAM) and 64-QAM transmission systems [20]. Meanwhile, the effects of EEPN have also been investigated in the orthogonal frequency division multiplexing (OFDM) transmission systems [22]. In our previous work, we have carried out a detailed analysis of the one-tap normalized least mean square (NLMS) carrier phase estimation method in the coherent system considering the impact of EEPN [23]. We have also proved that it is difficult to compensate the EEPN entirely, even using an optical reference carrier [24]. The EEPN scales with the increment of the fiber length, the symbol rate, and the LO laser linewidth [14-16], and it will significantly degrade the performance of the coherent optical communication systems. Involving the impact of EEPN, the traditional analysis for carrier phase estimation in coherent systems, where only pure laser phase noise are taken into account, may not be suitable again. Therefore, it is important to investigate in detail the performance of different carrier phase extraction methods in the coherent optical communication systems considering the EEPN.

In this paper, we present a comparative analysis on the performance of different carrier phase estimation methods in the coherent optical transmission system considering the equalization enhanced phase noise. Three carrier phase extraction algorithms, including a one-tap normalized least mean square method, a block-average (BA) method, and a Viterbi-Viterbi (VV) method are investigated for the phase noise mitigation in the *n*-level phase shift keying (*n*-PSK) coherent communication systems [10-13]. For the first time to our knowledge, the influence of EEPN is analyzed by using and comparing the analytical approximations and the simulation results of the three CPE methods. The numerical simulations are carried out in a 112-Gbit/s non-return-to-zero polarization division multiplexed quadrature phase shift keying (NRZ-PDM-QPSK) coherent transmission system, which is implemented in the VPI simulation platform [25]. The theoretical bit-error-rate (BER) floors in the three CPE methods including the impact of EEPN are calculated based upon the leading order of the Taylor expansion, which is the commonly used approach in the BER floor prediction for the CPE algorithms [26-28]. The theoretical predictions are compared to the practical simulation results. Meanwhile, the tolerable total effective linewidths (involving the TX, the LO lasers and the EEPN) in the three CPE methods with different block size are evaluated for a fixed BER floor, where the influence of the fiber nonlinearities are neglected. The computational complexity of the three carrier phase extraction methods is also discussed. Our analysis and discussions are useful and important for the practical design and application of the carrier phase estimation algorithms in long-haul high speed coherent optical transmission systems, where a large EEPN should be considered.

2. ANALYSIS FOR TOTAL PHASE NOISE VARIANCE CONSIDERING EEPN

In the coherent communication system with electronic CD equalization, the transmitter phase noise passes through both transmission fibers and the digital CD equalization module, and so the net dispersion experienced by the transmitter PN is close to zero. However, the local oscillator phase noise only goes through the electronic CD equalization module, and will be significantly enhanced due to the digital dispersion equalization [14-18].

The EEPN scales linearly with the accumulated chromatic dispersion and the linewidth of the LO laser, and the variance of the additional noise due to the EEPN can be expressed as follows, see e.g. [14,15]:

$$\sigma_{EEPN}^2 = \frac{\pi\lambda^2}{2c} \cdot \frac{D \cdot L \cdot \Delta f_{LO}}{T_S} \tag{1}$$

where λ is the central wavelength of the optical carrier wave, c is the light speed in vacuum, D is the CD

coefficient of the transmission fiber, L is the fiber length, Δf_{LO} is the 3-dB linewidth of the LO laser, and T_S is the symbol period of the transmission system.

Therefore, the total phase noise variance in the coherent transmission system including the EEPN can be expressed as:

$$\begin{aligned}\sigma^2 &= \sigma_{TX}^2 + \sigma_{LO}^2 + \sigma_{EEPN}^2 + 2\rho \cdot \sigma_{LO}\sigma_{EEPN} \\ &\approx \sigma_{TX}^2 + \sigma_{LO}^2 + \sigma_{EEPN}^2\end{aligned} \tag{2}$$

$$\sigma_{TX}^2 = 2\pi\Delta f_{TX} \cdot T_S \tag{3}$$

$$\sigma_{LO}^2 = 2\pi\Delta f_{LO} \cdot T_S \tag{4}$$

where σ^2 represents the total phase noise variance, σ_{TX}^2 and σ_{LO}^2 are the intrinsic phase noise variance of the TX and the LO lasers respectively, Δf_{TX} is the 3-dB linewidth of the TX laser, and ρ is the correlation coefficient between the EEPN and the intrinsic LO phase noise. We note that the approximation in Eq. (2) is valid when the transmission length for the normal single mode fiber exceeds the order of 80 km [23].

Corresponding to the definition of the intrinsic phase noise from TX and LO lasers, we employ an effective linewidth Δf_{Eff} to describe the total phase noise in the coherent system with EEPN [23,24], which can be defined as the following expression:

$$\begin{aligned}\Delta f_{Eff} &= \frac{\sigma_{TX}^2 + \sigma_{LO}^2 + \sigma_{EEPN}^2 + 2\rho \cdot \sigma_{LO}\sigma_{EEPN}}{2\pi T_S} \\ &\approx \frac{\sigma_{TX}^2 + \sigma_{LO}^2 + \sigma_{EEPN}^2}{2\pi T_S}\end{aligned}. \tag{5}$$

3. PRINCIPLE OF CARRIER PHASE ESTIMATION WITH EEPN

3.1 Principle of normalized LMS phase estimation

The one-tap NLMS filter can be employed effectively for carrier phase estimation [10], of which the tap weight is expressed as:

$$w(p+1) = w(p) + \frac{\mu}{|x(p)|^2} x^*(p) e(p) \tag{6}$$

$$e(p) = d(p) - w(p) \cdot x(p) \tag{7}$$

where $w(p)$ is the complex tap weight, $x(p)$ is the complex magnitude of the input signal, p represents the number of the symbol sequence, $d(p)$ is the desired symbol, $e(p)$ is the estimation error between the output signals and the desired symbols, and μ is the step size parameter.

The phase estimation using the one-tap NLMS filter resembles the performance of the ideal differential detection [23], and the BER floor for the *n*-PSK transmission systems using the one-tap NLMS carrier phase estimation can be approximately described by the following expression:

$$BER_{floor}^{NLMS} \approx \frac{1}{\log_2 n} erfc\left(\frac{\pi}{n\sqrt{2\sigma}}\right) \tag{8}$$

where σ is the square root of the total phase noise variance.

3.2 Principle of block-average phase estimation

The block-average method computes the *n*-th power of the symbols in each process unit to cancel the phase modulation, and the calculated phase are summed and averaged over the entire block (the length of the entire block is called block size). Then the phase is divided by *n*, and the result leads to a phase estimate for the entire block [11]. For the *n*-PSK transmission system, the estimated carrier phase for each process unit using the BA method can be expressed as:

$$\hat{\Phi}_{BA}(p) = \frac{1}{n} \arg\left\{ \sum_{k=1+(m-1)\cdot N_b}^{m\cdot N_b} x^n(k) \right\} \tag{9}$$

$$m = \left\lceil \frac{p}{N_b} \right\rceil \tag{10}$$

where N_b is the block size in the BA method, and $\lceil x \rceil$ represents the nearest integer larger than x.

Using a Taylor series expansion, the BER floor in the block-average carrier phase estimation for the *n*-PSK transmission system can be approximately expressed as follows - see e.g. [26,27]:

$$BER_{floor}^{BA} \approx \frac{1}{N_b \log_2 n} \cdot \sum_{k=1}^{N_b} erfc\left(\frac{\pi}{n\sqrt{2\sigma_{BA,k}}}\right) \tag{11}$$

$$\sigma_{BA,k}^2 = \frac{\sigma^2}{6N_b^2} \cdot \left[2(k-1)^3 + 3(k-1)^2 + 2(N_b - k)^3 + 3(N_b - k)^2 + N_b - 1\right],\ k=1,\ldots,N_b. \quad (12)$$

where σ^2 is the total phase noise variance.

3.3 Principle of Viterbi-Viterbi phase estimation

The Viterbi-Viterbi method also operates the symbols in each process unit into the *n*-th power to cancel the phase modulation. Meanwhile, the calculated phase are also summed and averaged over the entire block (the length of the block is also called block size). However, the difference with regard to the BA method is in the final step, where the extracted phase in the VV method is only concerned as the phase estimation for the central symbol in each block [12,13]. The extracted carrier phase in the *n*-PSK coherent transmission system using the Viterbi-Viterbi method can be expressed as:

$$\hat{\Phi}_{VV}(p) = \frac{1}{n}\arg\left\{\sum_{k=-(N_v-1)/2}^{(N_v-1)/2} x^n(p+k)\right\},\ N_v=1,3,5,7\ldots \quad (13)$$

where N_v is the block size in the VV method.

The phase estimation in the *n*-PSK coherent system using the Viterbi-Viterbi algorithm can also be analyzed by using the Taylor expansion [26-28], and the BER floor can be described by the following approximate expression:

$$BER_{floor}^{VV} \approx \frac{1}{\log_2 n} erfc\left(\frac{\pi}{n\sqrt{2}\sigma_{VV}}\right) \quad (14)$$

$$\sigma_{VV}^2 = \sigma^2 \cdot \frac{N_v^2 - 1}{12N_v} \quad (15)$$

where σ^2 is the total phase noise variance.

We can find that the carrier phase estimate error in Eq. (15) for the Viterbi-Viterbi method corresponds to the smallest phase estimate error (phase error in the central symbol) in Eq. (12) for the block-average method. Thus the Viterbi-Viterbi method will work better than the block-average method. Meanwhile, according to Eq. (8) and Eq. (14), the VV method will also show a better behavior than the one-tap NLMS method in theory, when the block size is less than 12. However, it requires more computational complexity to update the process unit for the phase estimation of each symbol.

3.4 Computational complexity

The computational complexity of the carrier phase extraction algorithms can be evaluated by the number of complex multiplications per symbol (Mul/Sym) and the block update efforts for each estimated symbol in the mitigation of the phase noise in the coherent transmission system. According to this description, the complexity of the three phase estimation methods in the *n*-PSK transmission system is calculated as the following expression:

$$C_{NLMS} = 3 + C_{update} \tag{16}$$

$$C_{BA} = n - 1 + C_{update} \tag{17}$$

$$C_{VV} = n - 1 + C_{update} \cdot N_v \tag{18}$$

where C_{NLMS}, C_{BA}, C_{VV} represent the computational complexity of the NLMS, the BA and the VV algorithms, respectively, and C_{update} denotes the update effort for each symbol in the data block. We note that the required multiplications for each estimated symbol in the VV method is not as the intuitive value $(n-1)\cdot N_v$, because we can reuse the *n*-th power calculation results of the previous block.

Roughly speaking, for the transmission systems with modulation level higher than QPSK ($n \geq 4$), the one-tap NLMS method will have the lowest computational complexity. The complexity of the BA and the VV algorithms scales linearly with the modulation level, while the VV method requires more efforts for updating the block and saving the *n*-th power calculation results in the previous block. Therefore, the VV algorithm usually requires more computational efforts than the other two methods.

3.5 Balance between phase noise and additive noise

The above descriptions for carrier phase estimation using the three algorithms are analyzed without involving the influence of the additive noise in the transmission channel, which should be considered for the practical optical communication systems. For the one-tap NLMS method, the step size parameter has an optimal value to achieve the best balance for the phase noise and the additive noise. In brief, a smaller step size will deteriorate the BER floor induced by the phase noise, while a larger step size will degrade the NLMS phase estimator on

the sensitivity of optical signal-to-noise ratio (OSNR). Hence, the step size parameter should be optimized for the practical use of the one-tap NLMS algorithm [10,23].

For the block-average and the Viterbi-Viterbi methods, an optimal block size should also be selected considering the balance of the phase noise and the additive noise. Generally speaking, a smaller block size will degrade the sensitivity of the OSNR in the coherent system [27], while a larger block size will degrade the BER floor induced by the phase noise according to Eq. (11) and Eq. (14). Therefore, we should consider the balance of the phase noise and the additive noise for the application of the three CPE methods in the practical transmission systems.

4. SIMULATION INVESTIGATION OF PDM-QPSK TRANSMISSION SYSTEM

As illustrated in Fig. 1, the simulation investigations have been carried out in the 112-Gbit/s NRZ-PDM-QPSK coherent transmission system based on the VPI simulation platform [25]. The data sequence output from the four 28-Gbit/s pseudo random bit sequence (PRBS) generators are modulated into two orthogonally polarized NRZ-QPSK optical signals by the two Mach-Zehnder modulators. Then the orthogonally polarized signals are integrated into one fiber channel by a polarization beam combiner (PBC) to form the 112-Gbit/s NRZ-PDM-QPSK optical signal. Using a local oscillator in the coherent receiver, the received optical signals are mixed with the LO laser to be transformed into four electrical signals by the photodiodes. The four electrical signals are processed by further using the Bessel low-pass filters (LPFs) with a 3-dB bandwidth of 19.6 GHz. Then they are digitalized by the 8-bit analog-to-digital convertors (ADCs) at twice the symbol rate [29]. The sampled signals are processed by the digital equalizers, and the BER is then estimated from the data sequence of 2^{17} bits. The central wavelength of the TX laser and the LO laser are both 1553.6 nm. The standard single mode fibers (SSMFs) with the CD coefficient equal to 16 ps/nm/km are employed in all the simulation work.

Here we neglected the influences of fiber attenuation, polarization mode dispersion and nonlinear effects in our simulation. The PMD and polarization rotation equalization could be realized by employing the adaptive LMS and constant modulus algorithm (CMA) equalizers [30,31]. The CD compensation is implemented by using a frequency domain equalizer (FDE) with appropriate parameters [32,33], which has been analyzed in our previous work [34].

With the increment of launched optical power, the fiber nonlinearities such as self-phase modulation (SPM), cross-phase modulation (XPM) and four-wave mixing (FWM) need to be considered in the long-haul wavelength-division multiplexing (WDM) transmission systems [2]. The fiber nonlinear impairments can be mitigated and compensated by using the digital backward propagation methods based on solving the nonlinear Schrodinger (NLS) equation and the Manakov equation [35,36].

Fig. 1. Scheme of 112-Gbit/s NRZ-PDM-QPSK coherent transmission system. PBS: polarization beam splitter, MZI: Mach-Zehnder interferometer, OBPF: optical band-pass filter, PIN: PiN diode, LPF: low-pass filter.

5. SIMULATION RESULTS

5.1 BER floors for BA and VV methods

In our previous report, we have compared the theoretical BER floors to the simulation results for the one-tap NLMS phase estimation, where a good agreement is always achieved [23]. Therefore, here we focus on the comparison between the theoretical BER floors and the practical simulations for the block-average and the Viterbi-Viterbi CPE methods, when a large EEPN exists in the coherent transmission system.

The performance of the BA carrier phase extraction method with different block size in the 112-Gbit/s NRZ-PDM-QPSK system is illustrated in Fig. 2. The transmission system is with 2000 km optical fiber, which means that there will be a considerable EEPN if the linewidth of LO laser is in the level of MHz. Here we use the FDE with 2048 fast Fourier transform (FFT) size and 1024 overlap for the CD compensation [34]. We note that different LO laser linewidths will lead to different EEPN variance, since the EEPN will scale linearly with the increment of LO laser linewidth. Hence, the EEPN in the case of “LO(only):10 MHz” will be the double of the EEPN in the case of “TX=LO=5 MHz”. We can find that for a small block size (N_b=3), the theoretical BER floors are much lower than the simulation results. Because for the minimum block size (N_b=1) in the BA algorithm, the theoretical prediction of the BER floor in Eq. (11) is zero. This indicates that Eq. (11) - which is based on a leading order Taylor expansion of the phase noise influence - is not accurate. A higher order Taylor approximation is required. Therefore, for a relative small block size (N_b=3), the theoretical BER floors will be

below the simulation results. For a large block size (N_b=11), the theoretical BER floor predictions are above the simulation results. Because the theoretical BER floor in the BA method is derived based on the Taylor expansion [26,27], which will not work well when both the block size (N_b=11) and the phase noise variance are large. A similar phenomenon has also been found in previous report [27]. Therefore, for a specific block size (N_b=5), the simulation results can make a good agreement with the theoretical predictions.

Fig. 2. Carrier phase estimation using BA method with different block size N_b. (a) N_b=3, (b) N_b=5, (c) N_b=11. The theoretical BER floor is 4.7×10^{-6} for the case of "TX=LO=5 MHz", which is too small to be shown in (a).

Figure 3 shows the performance of the VV carrier phase extraction method with different block size in the 112-Gbit/s NRZ-PDM-QPSK system, where the transmission fiber is also 2000 km (corresponding to a considerable EEPN, when the LO laser linewidth is several MHz). We also employ the FDE with 2048 FFT-size and 1024 overlap for the CD compensation [34]. A tendency similar to the BA method can be found in the VV phase estimation algorithm. For a small block size (N_v=5), the theoretical BER floors are lower than the simulation results. Because the minimum block size (N_v=1) in the VV method also corresponds to a zero BER floor in Eq. (14). This indicates that Eq. (14) - based on a leading order Taylor expansion of the phase noise - is not accurate either. A higher order Taylor approximation is required. Therefore, for a relative small block size (N_v=5), the theoretical BER floors will be below the simulation results. For a large block size (N_v=15), the theoretical predictions of the BER floor are above the simulation results. This is because a large block size (N_v=15) and a large phase noise variance could not achieve a good approximation in the Taylor expansion for the theoretical calculation of BER floor in Eq. (14) [26-28]. Similar to the BA method, the simulation results could agree well with the theoretical predictions for a specific block size (N_v=11). We can find that the specific block size (simulation results matching the theoretical predictions) in the BA method is smaller than in the VV method.

Fig. 3. Carrier phase estimation using VV method with different block size N_v. (a) N_v=5, (b) N_v=11, (c) N_v=15. The theoretical BER floor is 1.5×10^{-7} for the case of "TX=LO=5 MHz", which is too small to be shown in (a).

As discussed in the above, the analytical evaluation of the BER floors in the BA and the VV carrier phase extraction methods is derived based on the Taylor expansions. However, Taylor expansion methods - to the

leading order in the phase noise – are not accurate for the large phase noise and block size values. In most practical cases, the BA and the VV algorithms allow the large phase noise (such as EEPN) and block size parameters, and the Taylor expansion based analytical predictions are not appropriate. Therefore, a proper analysis for the practical transmission system should be described based upon the simulation results.

5.2 Comparison of three carrier phase extraction methods

The performance of three carrier phase estimation algorithms with different block size is illustrated in Fig. 4. The transmission fiber length is 2000 km, and the TX and the LO linewidths are both 5 MHz, therefore, a significant EEPN should be considered. The FDE with 2048 FFT-size and 1024 overlap is employed for the CD compensation. The step size in the one-tap NLMS algorithm is optimized. For the one-tap NLMS method, the theoretical BER floor always makes a good agreement with the simulation result, if the step size is optimized. When the block size is one, the BA algorithm shows exactly the same behavior with the VV algorithm, which is a little better than the one-tap NLMS method. Meanwhile, as described in the Section 5.1, the theoretical prediction of the BER floors matches the simulation results, only if the block size is 5 for the BA method and the block size is 11 for the VV method. Furthermore, we can find that the VV method shows a small improvement than the BA method. In the case of BER=10^{-3} and block size N_b=N_v=5, we can find that the OSNR improvement is around 1 dB. This improvement comes from the smaller carrier phase estimate error in the VV method compared to in the BA method.

Fig. 4. Performance of three CPE methods with different block size, where the fiber length is 2000 km, and the TX and the LO linewidths are both 5 MHz. (a) block size is 1, (b) block size is 5, (c) block size is 11. The theoretical BER floor is 1.5×10^{-7} for the VV method, which is too small to be shown in (b).

Figure 5 indicates the tolerable total effective linewidth for the three carrier phase extraction methods with different block size in the 112-Gbit/s NRZ-PDM-QPSK coherent transmission system. Figure 5(a) is the theoretical evaluation, and Fig. 5(b) is the numerical simulation result. According to the theoretical prediction in Fig. 5(a), we can find that the block size has a significant influence on the performance of the BA and the VV methods. The BA and the VV methods degrade dramatically with the increment of the block size. The BA method is much better (allowing larger effective linewidth) than the NLMS method with the block size less than

5, and the VV method is much better than the NLMS method with the block size less than 13. Meanwhile, the VV method gives a much better behavior than the BA method. However, the simulation results in Fig. 5(b) demonstrate that the BA and the VV methods have a weaker dependence on the block size compared to the theoretical analysis. On the one hand, the BA method behaves a little better (allowing larger effective linewidth) than the NLMS method when the block size is less than 11, and the VV method works slightly better than the NLMS method when the block size is less than 21. On the other hand, the Viterbi-Viterbi method shows only a small improvement compared to the block-average method, even if it sacrifices more computational complexity.

Fig. 5. Maximum tolerable effective linewidth for different BER floors (10^{-2}, 10^{-3}, 10^{-4}) in the three methods versus the block size. (a) theoretical predictions, (b) simulation results.

The weak dependence on the block size in the BA and the VV algorithms implies that the additive noise in the transmission channel of the practical coherent systems can be accommodated quite well, since this requires a large block size to mitigate the additive Gaussian noise. Meanwhile, the NLMS method can also show a good performance with the additive noise in the transmission channel, if the step size is optimized [10,23].

It is worth noting that the one-tap NLMS algorithm can also be employed for the *n*-QAM coherent transmission systems, while the block-average and the Viterbi-Viterbi methods can not be easily used for the classical *n*-QAM coherent systems except the circular constellation *n*-QAM systems.

6. CONCLUSIONS

In this paper, the performance of different carrier phase extraction methods is comparatively investigated in the high speed coherent optical communication systems considering the impact of equalization enhanced phase noise. Three approaches, involving the one-tap NLMS algorithm, the block-average algorithm and the Viterbi-Viterbi algorithm are applied for the carrier phase extraction in the *n*-level PSK coherent transmission system. The simulation work is performed in the 112-Gbit/s NRZ-PDM-QPSK coherent optical transmission system, where the chromatic dispersion is compensated by the fixed frequency domain equalizer. The analytical bit-error-rate floors in the three carrier phase estimation methods considering the influence of EEPN are evaluated based upon the commonly used Taylor expansion. The theoretical predictions are compared to the practical simulation results. The complexity of the three CPE methods is also discussed. The theoretical

predictions of the BER floors in the NLMS phase estimation method always make a good agreement with the simulation results, while it is not the case for the block-average and the Viterbi-Viterbi methods, where the leading-order Taylor expansion based theoretical BER floors only match the simulation results when a specific block size is employed. The numerical simulations also demonstrate that the effects of the block size on the block-average and the Viterbi-Viterbi methods are much weaker than what is presented by the traditional theoretical evaluation, when the EEPN is considered.

For the design of practical transmission systems, simulations should be applied for the evaluation of the three carrier phase estimation methods. The one-tap NLMS method can show an acceptable behavior compared to the other two approaches, while the optimization for the step size needs a complicated empirical selection. The block-average method is easy and efficient to implement, but it will behave unsatisfactorily when a large block size is used. The Viterbi-Viterbi method can show a small improvement compared to the block-average method, while it requires more computational complexity for updating the data block than the other two methods.

To focus on the influence of EEPN in carrier phase estimation, we have neglected the impact of the fiber nonlinearities in our simulation work for evaluating the BER floors and the tolerable total effective linewidths in coherent transmission system. It would be more complicated if we consider the influence of the fiber nonlinearities, because the electronic CD equalization could also interact with the fiber nonlinear effects [19]. Further analysis for carrier phase estimation algorithms involving both the EEPN and the fiber nonlinear effects will be investigated in our future work.

REFERENCES

[1] P. S. Henry, IEEE J. Quantum Electron. 21 (1985) 1862-1879.

[2] G. P. Agrawal, Fiber-optic communication systems, third ed., John Wiley & Sons, Inc., New York, 2002.

[3] H. Bulow, F. Buchali, A. Klekamp, J. Lightwave Technol. 26 (2008) 158-167.

[4] T. Merker, N. Hahnenkamp, P. Meissner, Opt. Commun. 182 (2000) 135-141.

[5] Y. Gao, F. Zhang, L. Dou, Z. Y. Chen, A. S. Xu, Opt. Commun. 282 (2009) 992-996.

[6] X. Zhou, J. Yu, D. Qian, T. Wang, G. Zhang, P. D. Magill, J. Lightwave Technol. 27 (2009) 146-152.

[7] E. Ip, A. P. T. Lau, D. J. F. Barros, J. M. Kahn, Opt. Express 16 (2008) 153-791.

[8] S. J. Savory, Opt. Express 16 (2008) 804-817.

[9] M. G. Taylor, J. Lightwave Technol. 17 (2009) 901-914.

[10] Y. Mori, C. Zhang, K. Igarashi, K. Katoh, K. Kikuchi, Opt. Express 17 (2009) 1435-1441.

[11] D. S. Ly-Gagnon, S. Tsukamoto, K. Katoh, K. Kikuchi, J. Lightwave Technol. 24 (2006) 12-21.

[12] C. R. S. Fludger, T. Duthel, D. V. D. Borne, C. Schulien, E. D. Schmidt, T. Wuth, J. Geyer, E. D. Man, G. D. Khoe, H. D. Waardt, J. Lightwave Technol. 26 (2008) 64-72.

[13] A. Viterbi, IEEE Trans. Inf. Theory 29 (1983) 543-551.

[14] W. Shieh, K. P. Ho, Opt. Express 16 (2008) 15718-15727.

[15] A. P. T. Lau, W. Shieh, K. P. Ho, Proc. OptoElectron. Commun. (OECC' 2009), FQ3.

[16] A. P. T. Lau, T. S. R. Shen, W. Shieh, K. P. Ho, Opt. Express 18 (2010) 17239-17251.

[17] K. P. Ho, A. P. T. Lau, W. Shieh, Opt. Lett. 36 (2011) 585-587.

[18] C. Xie, Proc. Conf. Opt. Fiber Commun. (OFC' 09), OMT4.

[19] C. Xie, Opt. Express 17 (2009) 4815-4823.

[20] I. Fatadin, S. J. Savory, Opt. Express 18 (2010) 16273-16278.

[21] S. Oda, C. Ohshima, T. Tanaka, T. Tanimura, H. Nakashima, N. Koizumi, T. Hoshida, H. Zhang, Z. Tao, J. C. Rasmussen, Proc. Euro. Conf. Opt. Commun. (ECOC' 2010), Mo.1.C.2.

[22] Q. Zhuge, C. Chen, D. V. Plant, Opt. Express 19 (2011) 4472-4484.

[23] T. Xu, G. Jacobsen, S. Popov, J. Li, A. T. Friberg, Y. Zhang, Opt. Express 19 (2011) 7756-7768.

[24] G. Jacobsen, T. Xu, S. Popov, J. Li, A. T. Friberg, Y. Zhang, Opt. Express 19 (2011) 14487-14494.

[25] www.vpiphotonics.com

[26] S. Benedetto, E. Biglieri, V. Castellani, Digital transmission theory, Prentice-Hall, Inc., New Jersey, 1987.

[27] E. Vanin, G. Jacobsen, Opt. Express 18 (2010) 4246-4259.

[28] G. Jacobsen, J. Opt. Commun. 31 (2010) 180-183.

[29] S. J. Savory, Proc. Conf. Opt. Fiber Commun. (OFC' 08), OTuO3.

[30] K. Kikuchi, Opt. Express 19 (2011) 9868-9880.

[31] D. S. Millar, S. J. Savory, Opt. Express 19 (2011) 8533-8538.

[32] M. Kuschnerov, F. N. Hauske, K. Piyawanno, B. Spinnler, A. Napoli, B. Lankl, Proc. Conf. Opt. Fiber Commun. (OFC' 09), OMT1.

[33] R. Kudo, T. Kobayashi, K. Ishihara, Y. Takatori, A. Sano, Y. Miyamoto, J. Lightwave Technol. 27 (2009) 3721-3728.

[34] T. Xu, G. Jacobsen, S. Popov, J. Li, E. Vanin, K. Wang, A. T. Friberg, Y. Zhang, Opt. Express 18 (2010) 16243-16257.

[35] G. Goldfarb, M. G. Taylor, G. Li, IEEE Photon. Technol. Lett. 20 (2008) 1887-1889.

[36] F. Yaman, G. Li, IEEE Photonics J. 1 (2009) 144-152.

Figure Captions

Fig. 1. Scheme of 112-Gbit/s NRZ-PDM-QPSK coherent transmission system. PBS: polarization beam splitter, MZI: Mach-Zehnder interferometer, OBPF: optical band-pass filter, PIN: PiN diode, LPF: low-pass filter.

Fig. 2. Carrier phase estimation using BA method with different block size N_b. (a) N_b=3, (b) N_b=5, (c) N_b=11. The theoretical BER floor is 4.7×10^{-6} for the case of "TX=LO=5 MHz", which is too small to be shown in (a).

Fig. 3. Carrier phase estimation using VV method with different block size N_v. (a) N_v=5, (b) N_v=11, (c) N_v=15. The theoretical BER floor is 1.5×10^{-7} for the case of "TX=LO=5 MHz", which is too small to be shown in (a).

Fig. 4. Performance of three CPE methods with different block size, where the fiber length is 2000 km, and the TX and the LO linewidths are both 5 MHz. (a) block size is 1, (b) block size is 5, (c) block size is 11. The theoretical BER floor is 1.5×10^{-7} for the VV method, which is too small to be shown in (b).

Fig. 5. Maximum tolerable effective linewidth for different BER floors (10^{-2}, 10^{-3}, 10^{-4}) in the three methods versus the block size. (a) theoretical predictions, (b) simulation results.

Figure1

Click here to download high resolution image

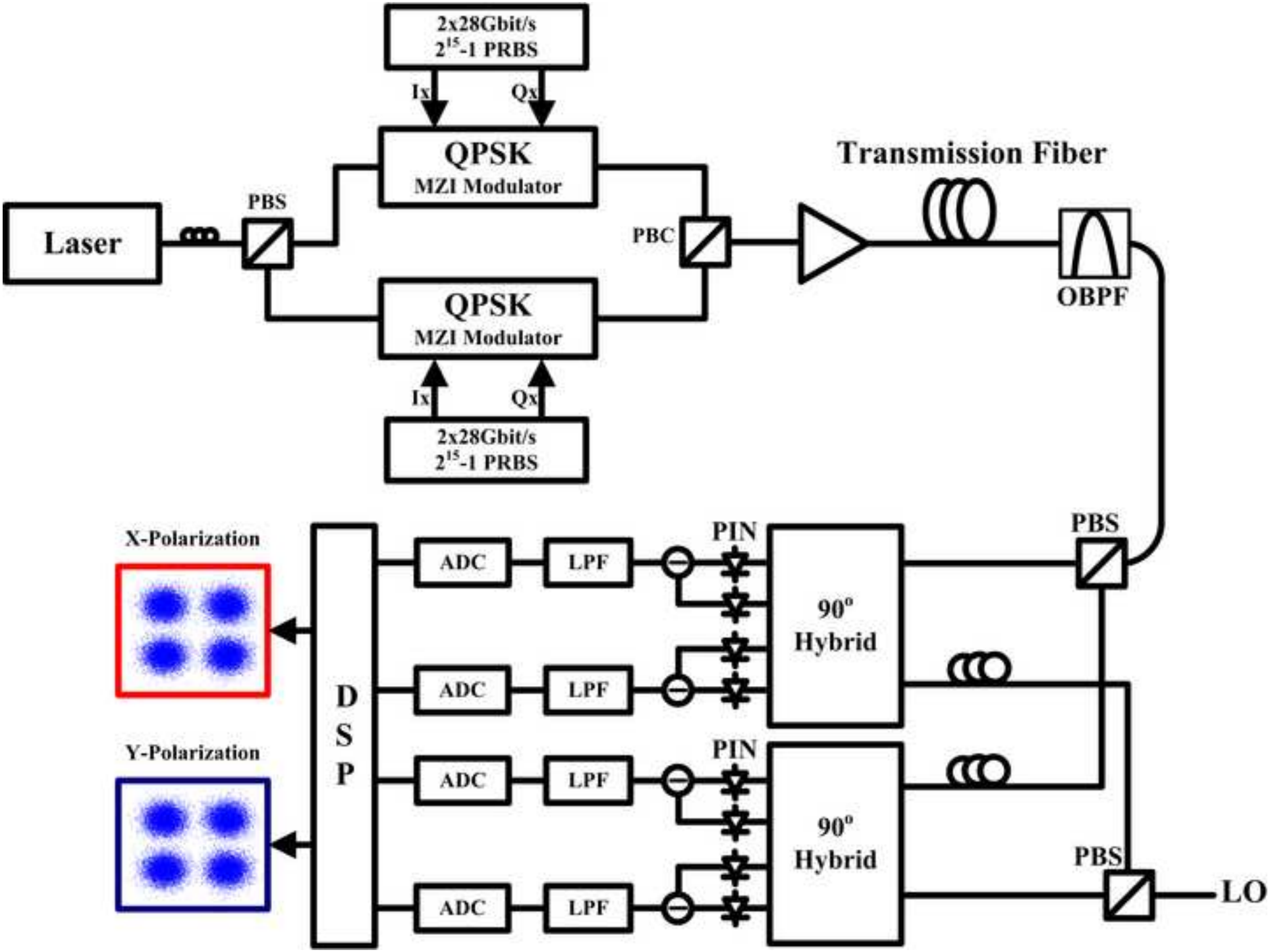

Figure2

Click here to download high resolution image

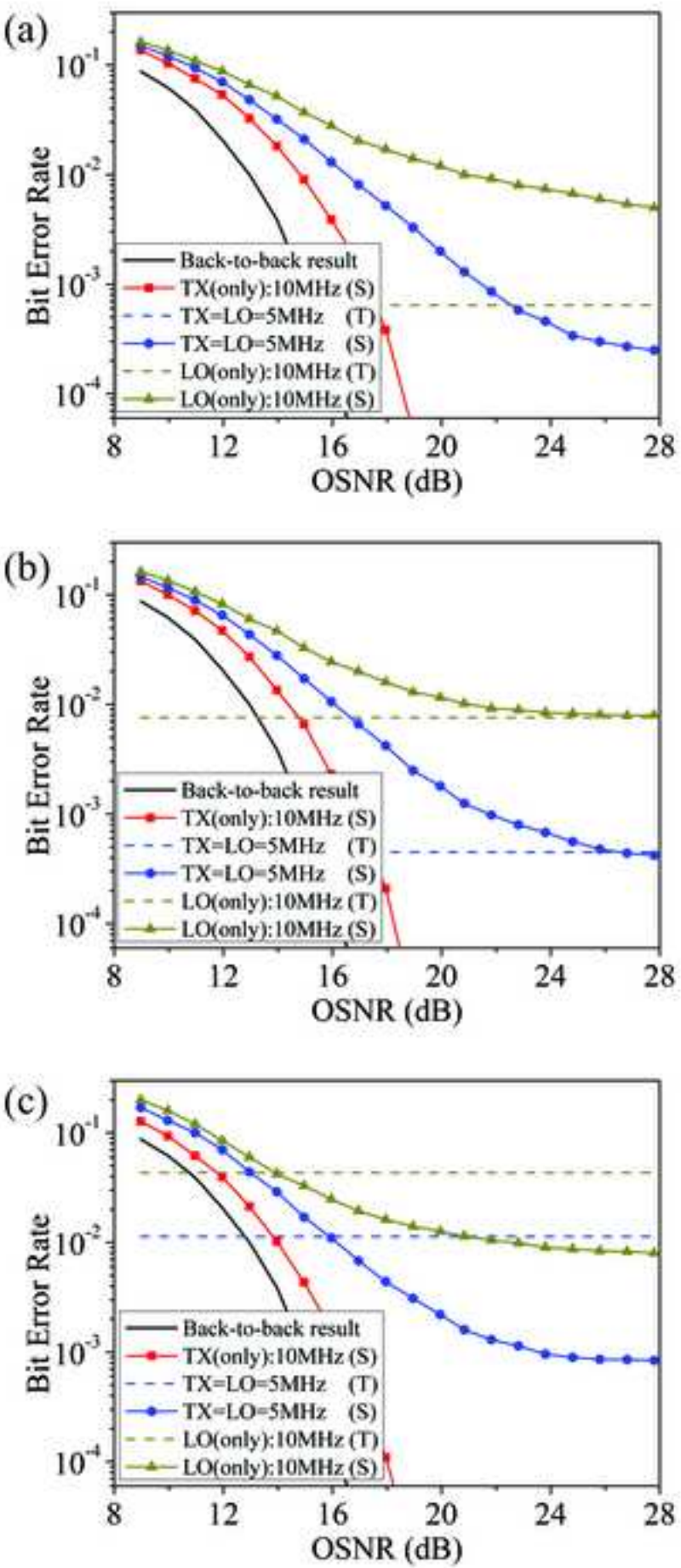

Figure3

Click here to download high resolution image

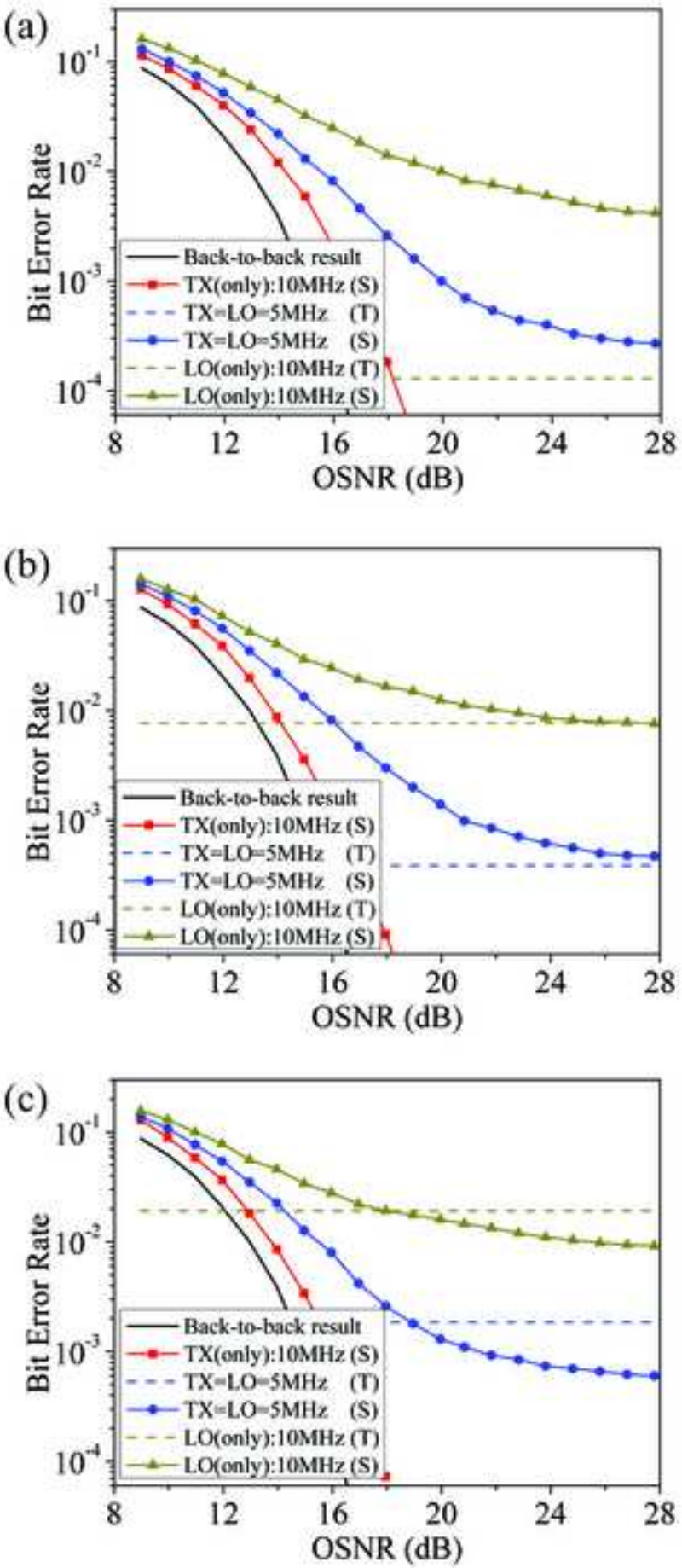

Figure4
Click here to download high resolution image

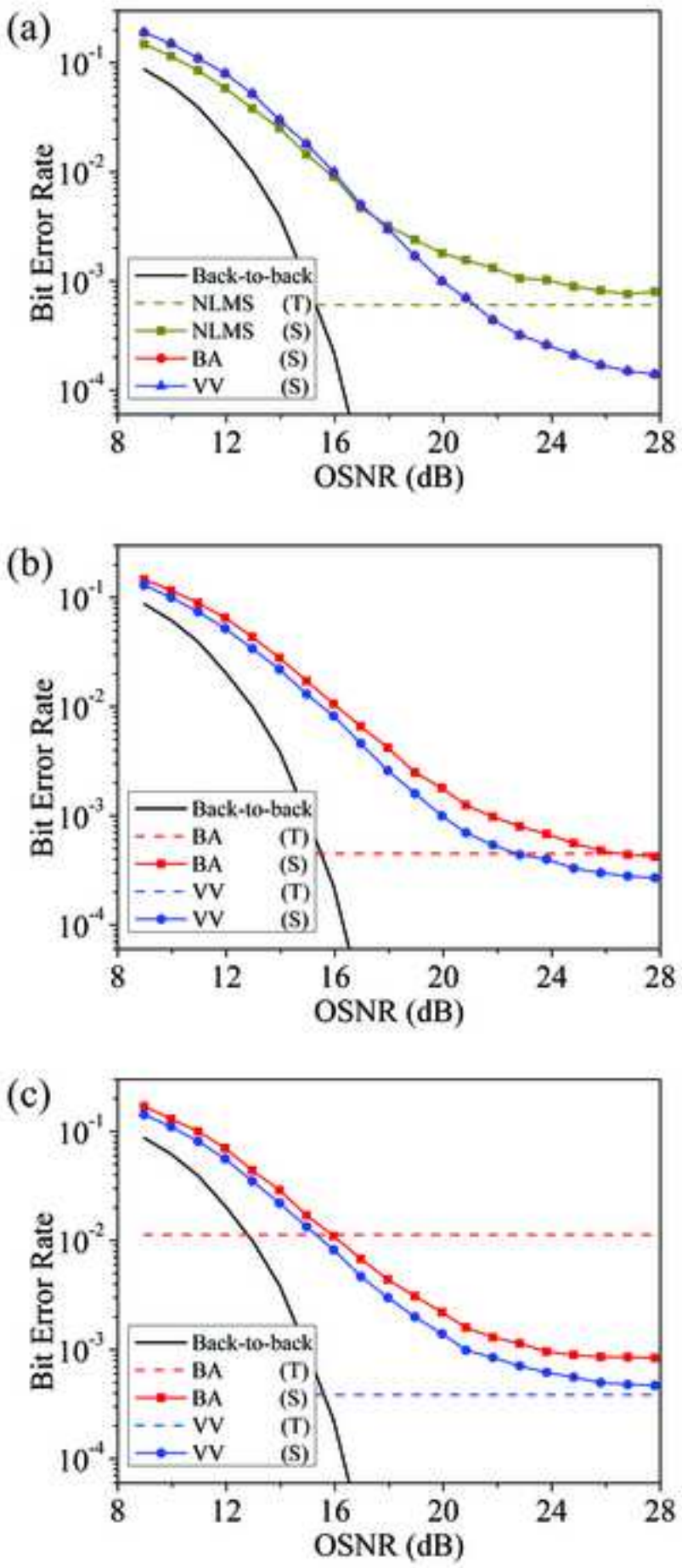

Figure5
Click here to download high resolution image